NVH optimization methodologies based on bead modification analysis in vehicle body design

A. Maressa[1], B. Pluymers[1], S. Donders[2], W. Desmet[1]

[1] K.U.Leuven, Department Mechanical Engineering, Division PMA
Celestijnenlaan 300 B – box 2420, B-3001, Heverlee, BELGIUM
e-mail: **antonio.maressa@mech.kuleuven.be**

[2] LMS International, CAE Division
Interleuvelaan 68, B-3001, Leuven, BELGIUM

Abstract

Nowadays, in automotive industry the vehicle design cycle is mainly ruled by the highly competitive nature of the market and the ever increasing customer demands and expectations. This challenges automotive manufacturers to achieve higher-quality products in ever shorter time frames, while at the same time, reduce the design costs. This can only be achieved when the design cycle takes place largely on the basis of virtual modeling and simulation such that the traditional test phase, which relies on expensive and time-consuming physical prototypes, can be drastically shortened. As a result, nowadays, each stage of the design cycle is supported by CAE (Computer Aided Engineering) methodologies which allow to predict various functional performance attributes, such as NVH (Noise, Vibration & Harshness), crashworthiness, etc. Moreover, researchers have developed many techniques to speed up the calculations, enabling efficient modification approaches and optimizations.

This paper focuses on the vehicle interior NVH performance. For a vehicle body Finite Element (FE) model, a reduced formulation has been achieved by using the WBS (Wave-Based Substructuring) technique. More specifically, a modification approach has been applied that is based on the generation of bead patterns on a subcomponent that has been identified as critical for the NVH behavior. By combining the reduced structural model with an efficient ATV (Acoustical Transfer Vector) approach to predict the interior acoustics performance, one can efficiently evaluate the effect of structural modifications on the interior NVH levels, such that the global NVH behavior can be optimized. The main innovation introduced in this paper comprises the optimization of vehicle vibro-acoustics by making use of a structural optimization software in combination with an acoustic target function. Two different methodologies have been worked out, based on two strategies for bead pattern optimization. Finally, the optimized component has been evaluated in terms of radiated Sound Pressure Level (SPL) and manufacturability.

1 Introduction

In automotive industry, the ever increasing customers' demands and the pressure from the highly competitive market push the design engineers to create better products faster and at lower costs [1]. This can only be achieved with innovative engineering solutions. For this purpose, CAE methodologies are used more and more, enabling a virtual development cycle with lower costs and elapsed time of the design cycle. When the vehicle design can be optimized in a virtual design engineering process, one can eliminate expensive "Test, Analyze & Fix" phases through physical prototypes [2], and take important design decisions earlier and at a lower cost [3,4].

Nowadays, automotive OEMs (i.e. Original Equipment Manufacturers) aim at a "Design Right First Time" process [5,6] in which only a single prototype is manufactured to validate the design before the

start of production. The only way to achieve this is to frontload the development process with Functional Performance Engineering (FPE) - to get engineering problems solved as early as possible in the design cycle and this at lower costs. For this purpose, a simulation-based design process must be achieved, in which simulation is the primary means of design evaluation and verification [4]. This goal can be reached only when the bottlenecks are solved at each design phase [7]. In this paper, the vehicle functional performance attribute of interest is the Noise, Vibration and Harshness (NVH) behavior. The current trends in automotive NVH design are focused on mass customization: a higher number of variants is developed on a lower number of platforms [8].

In the automotive NVH simulation process, a number of challenges can be distinguished. Firstly, the requirement for accurate predictions in the medium frequency gap in between FE (Finite Element) methods and SEA (Statistical Energy Analysis) [29]. One approach here is to use an FE strategy up to higher frequencies, which requires model reduction, improved structural modeling techniques (for connectors, trim, damping, …) and the assessment of the effect of uncertainty on the vehicle response. The second challenge is to make NVH predictions become available earlier in the design process, to allow improving the quality of the initial design and to increase the feasibility to balance possibly conflicting performance attributes (e.g. NVH, fuel economy and crash/safety) [9]. The final challenge is that faster design iterations are needed, to allow the evaluation of more variants / enable a larger-scale optimization / enable a more extensive uncertainty assessment in a given time. By focusing on CAE technologies for efficient vibro-acoustic analysis of vehicles, this paper addresses the third challenge, aimed at faster design iterations towards modifying and improving the vehicle NVH performance.

The main innovation reported in this paper is using a combination of existing FE tools for structural analyses and optimizations with an acoustic target function, aimed at optimizing the vibro-acoustic performances of a vehicle. Three advanced FE methodologies will be combined; namely the WBS (Wave-Based Substructuring) method, the ATV (Acoustic Transfer Vector) approach and so-called Bead-Based Structural Optimization. The WBS approach allows creating a fast and accurate reduced structural model, which can be used to efficiently calculate the impact of structural modifications (in this paper bead modifications) on the structural dynamics performance. The robustness of the wave-based assembly model to local modifications has been validated [7,10]. When combined with the ATV approach, one can evaluate the impact of structural modifications on the interior NVH levels in a weakly coupled manner.

Section 2 reports on the numerical methods that are used to achieve the assembly-level FE model and to assess its interior NVH performance. The nominal case and the process for achieving the WBS-reduced FE model are described in Section 3. In Section 4, the different bead pattern optimization strategies are reported and applied on a vehicle-like case study. The paper is concluded in Section 5.

2 Numerical methods – Theory and applications

In the previous Section, a general outline of the work has been provided and the main issues have been introduced. In this section, a number of numerical methods are introduced, which are used together to establish a process for optimizing the interior vehicle NVH performance by means of virtual prototyping optimization. The first step consists in identifying a critical component in terms of interior acoustics radiation, which can subsequently be modified to improve the global vehicle interior NVH performance.

As one is dealing with large-sized FE models, Domain Decomposition and Component Mode Synthesis are used to achieve a simplified representation of the original mode [21]. Wave-Based Substructuring is used for an efficient representation of the interface between substructures, enabling fast accurate assembly-level analyses that can be used in an optimization scenario [22,30].

The global structural dynamic response of a vehicle-like structure is modified by applying purely geometrical modifications on the radiating panel. More specifically, so-called bead patterns are created by using algorithms that are available in commercial optimization software [25]. Finally the NVH behavior of the assembly-level model is assessed in terms of acoustic pressure by means of the Acoustic Transfer Vector approach.

2.1 Wave-Based Substructuring (WBS)

Substructuring methods are based on the domain decomposition of a complete (FE) structure into several substructures, which are independently solved at a sub-component level. An alternative representation of the original model is finally achieved by recombining the substructures into an assembly level model.

In substructuring, one approach is to use a reduced modal model of a structure, by representing the physical DOFs of each substructure into a reduced number of so-called generalized coordinates. Different modal-based methods have been reported [11-15], in which the generalized coordinates consist of the substructure natural modes (under some boundary conditions) and static enrichment modes (to accurately represent the local flexibility at the connection interface). In the approach by MacNeal & Rubin [14,15], static enrichment vectors are calculated to accurately represent the local flexibility at the connection interface DOFs. These static vectors are included in the mode set as artificial "mode shapes", which contain the local flexibility at 0Hz and which have a resonance frequency at a much higher frequency than the maximum frequency for the structural analysis.

Traditionally one has to obtain an enrichment vector for each interface DOF onto the assembly-level component, which becomes prohibitively costly for complex industrial models with extensive interfaces between adjacent substructures (e.g. weather strips, spot welds between floor and body). To address this, a Wave-Based Substructuring approach has been developed [16,17], in which the deformation of the coupling interface is written as a linear combination of a set of basis functions called "waves".

The calculation of these basis functions requires a modal analysis on the nominal FE model, performed in free-free boundary conditions, such that the 6 rigid body modes are also obtained. The mathematical treatment of a limited number of the first global modes, by means of a Singular Value Decomposition, enables the calculation of a set of orthonormal basis functions. In the WBS approach, connections between substructures (classically defined in terms of interface DOFs) are replaced by connections between wave DOFs that impose the continuity of displacements and forces. The required number of wave DOFs for an accurate coupling of substructures is much lower than the number of physical interface DOFs, which results in a smaller-sized assembly definition. This greatly facilitates the reduction procedure for large components, since a much lower number of enrichment vectors must be calculated, now defined in terms of wave participation factors.

The wave calculation is case-dependent, but the nominal wave set is rather robust for typical applications, and can also be used to connect modified components into the assembly structure, as has been demonstrated in Donders et al [17]. After a nominal assembly model has been defined using WBS, local modifications on components in FE representation can be processed quickly to predict the updated structural dynamics performance.

2.2 Bead pattern as structural modification

A modern automotive vehicle body consists of a large number of panels (e.g. doors, windshield, roof, spare wheel panel, floor, …). An important geometric feature of such components is that one of the dimensions (i.e. the thickness) is much smaller-sized than the other dimensions, leading to a two-dimensional panel structure with two-dimensional plane behavior. In Finite Element modeling, one can model panels with shell elements. Due to the low curvature and wide dimensions, large-amplitude vibrations occur that strongly affect the interior vibro-acoustic comfort of a vehicle. In order to reduce the vibration energy level and the radiated noise, structural modifications can be applied to the panels.

Bead modifications can be seen as a subset of mesh morphing [26]. In bead modification, only the nodal positions of the shell nodes are used as design variables, as shown in Figure 1. After deciding a suitable bead pattern in a virtual environment, one can apply the bead shape on a physical structure by using a dedicated manufacturing technique such as a deep-drawing process.

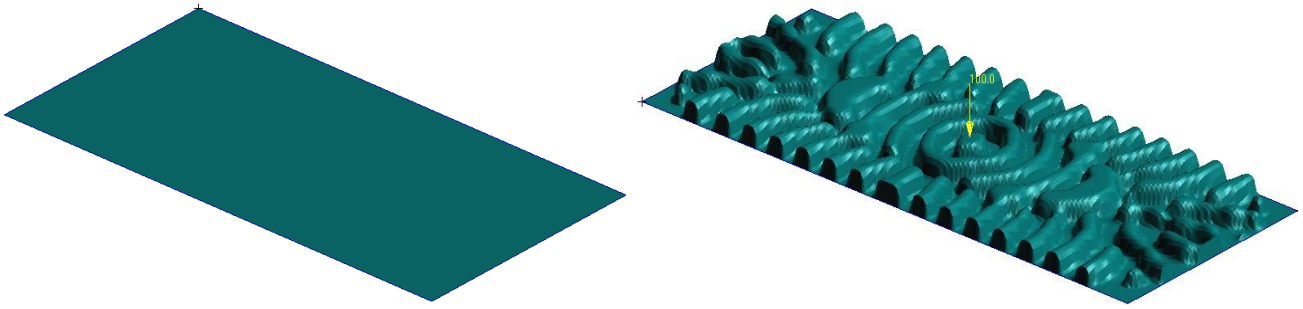

Figure 1. Bead-based modifications on a simple plate (100x40x1 mm).
Original FE model (left) and beaded version (right)

As shown in Figure 1, a bead pattern is obtained by dragging a selected set of nodes along the direction parallel to the local normal vector. This yields to a much stiffer panel as the bending stiffness increases with the third power of the distance to the neutral plane. However, the increment on the bending stiffness is not the only dynamic effect, since a moderate increment of mass is also involved due to the increment of the surface of the shell area. Beading is particularly suitable for two dimensional components which are mainly subject to bending stress but it might result in a weakening effect for the membrane stiffness [26].

In the re-design phase of industrial components, the key value of bead patterns is that they lead to a much stiffer component under bending stress, which is often the best way to reduce vibrations and hence the acoustics radiation. In a virtual engineering process, beads are usually created by means of an optimization software that applies a bead pattern according to a structural objective function (e.g. eigenfrequencies, compliance, etc). This paper presents results obtained with the Tosca 7.0.1 software [25], where bead-based modifications are performed by using two different algorithms, namely a Controller-based and a Sensitivity-based approach.

2.2.1 Controller-based algorithm

One approach to create bead patterns is to rely on the so-called Controller-based algorithm which makes use of bending stress evaluation results to decide on the most suitable bead pattern. The controller based algorithm consists of two steps. During the first step the Differential Bending Stress [26] is analyzed with the aim of obtaining the direction along which the stress is increasing, as shown in Figure 2 a). The second step then consists in applying a bead filter algorithm, which directly allows generating beads along the bending trajectories, as shown in Figure 2 b).

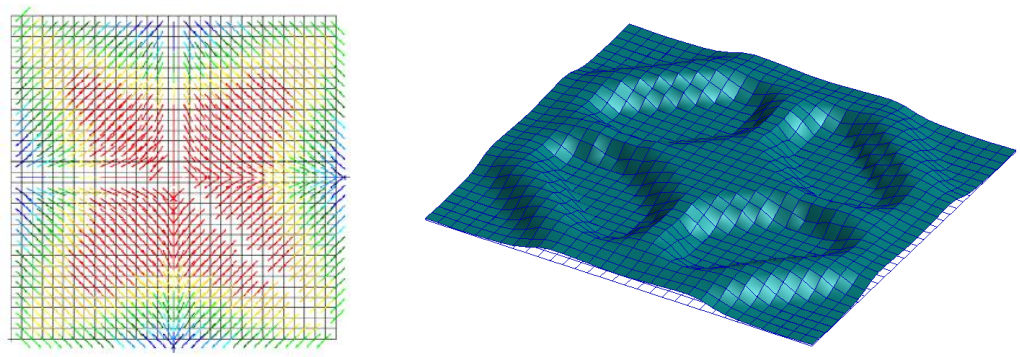

Figure 2. Controller Based Algorithm. Case study: square-shaped plate [25, 26].
a) Bending Stress Tensor (left) and b) resultant bead pattern (right)

The controller algorithm starts from user inputs to allow some control on the geometrical features of the created beads (i.e. height and width). It is fast and efficient since only a small number of iterations is required for the algorithm to converge to a suitable bead pattern. The bead pattern generation can be performed on the basis of compliance results for linear static analyses and eigenfrequencies results for dynamic problems. This paper reports on cases in which a physical bead pattern is obtained by maximizing the eigenfrequency values of a selected set of natural modes.

The fact that the generated patterns are only based upon the bending stress does not allow reaching the best solution in all cases as the membrane stiffness might be locally reduced.

2.2.2 Sensitivity-based algorithm

A second algorithm for bead optimization is the so-called Sensitivity based Algorithm [25]. By performing a number of sensitivity analyses, a selection is made of the most suitable nodal configuration according to the objective function [31]. For each iteration a fixed number of mesh perturbations (usually about 10) is generated [32], such that a wide part of the design space can be explored.

Sensitivity analyses are rather time consuming but, at the same time, allow obtaining accurate results as the updating procedure of the nodal positions is based upon the effective influence on the objective function. The generated mesh configurations are quite smooth and often a rather unclear bead pattern is generated, as the updating procedure of the nodal positions does not include a bead filter (which ensures that the nodal position modifications are tuned to have a bead shape, cfr. the bead-controller algorithm). However, the sensitivity based bead solutions most often yield less numerical issues in terms of distorted meshes and yield better/easier manufacturability.

The optimizations based on sensitivity analyses can rely on a wide number of objective functions and parameters, based on most of the types of structural analysis, including Modal Based Forced Responses.

2.3 Acoustic Transfer Vector approach

The main purpose of the presented work is to improve the interior vibro-acoustic comfort of industrial vehicles. The acoustic performances are virtually measured in terms of acoustic pressures at certain positions (i.e. virtual driver ear position), while the source is a purely mechanical (frequency-dependent) load, simulating the engine vibrations.

The physical problem is given by the coupling between a vibrating structural domain and a closed acoustic domain. In most of the common applications in automotive industry the acoustic fluid is air, which allows approximating the problem as weakly coupled. This way both problems are solved independently as uncoupled. More exactly, first the acoustic response is calculated and, in the last step, the structural velocities are imposed as boundary conditions for the uncoupled acoustic problem.

Based the hypothesis previously shown, is the Acoustic Transfer Vector approach which consists in calculating the acoustic pressure at certain locations starting from the normal velocity field acting on the acoustic boundaries [18], according to Eq. (1).

$$p(f) = \{ATV(f)\}^T \cdot \{v_n(f)\} \tag{1}$$

where $p(f)$ is representing the acoustic pressure at frequency f and it is written as linear function of the normal velocities acting on the nodes of the acoustic domain. The term $\{ATV(f)\}$ denotes the Acoustic Transfer Vector; the *j*th element represents the acoustic pressure response that is obtained when a unit normal velocity is applied on node *j*. As such, the acoustic transfer vector depends on the geometry of the acoustic domain, the fluid properties and the location of the virtual microphone (where the acoustic pressure is requested). The nominal ATV matrix can thus be calculated only once for a given interior acoustic cavity setup, and – when structural modifications (with limited geometrical changes) are made –

the nominal ATV matrix can be re-used to propagate the modified structural responses into the acoustic cavity so that the updated acoustic pressure levels are obtained efficiently.

In the design cycle of automotive structures, it is common to deal with the modal response of the body, in terms of both natural frequencies and modal shapes (often calculated in free-free conditions). Provided that the modal behavior is known and by introducing the modal superposition, Eq. (1) can be re-written as follows:

$$p(\omega) = \{MATV(\omega)\}^T \cdot \{q(\omega)\} \tag{2}$$

where $\{MATV(\omega)\}$ is the Modal Acoustic Transfer Vector as function of the angular frequency ω, and $\{q(\omega)\}$ represents the vector containing the modal participation factors.

$$\{MATV(\omega)\}^T = \{ATV(\omega)\}^T \cdot i \cdot \omega \cdot [\Phi_n] \tag{3}$$

By applying the previous transformation the acoustic pressure, an equation is obtained which is typically characterized by a much smaller set of parameters – since typically only a very limited number of structural modes are required, as compared to the number of structural response point at the wetted surface (i.e. the structural surface that consists of nodes that radiate into the acoustic cavity). The physical meaning of a MATV component is the pressure at the virtual microphone position when the correspondent mode is applied as boundary condition. Eq. (3) shows the definition of the MATV, where $[\Phi_n]$ contains as columns the natural modes projected in the direction that is normal to the acoustic boundaries.

3 Case description

Section 2 gives a brief introduction of the numerical methods and techniques applied in order to calculate the vibro-acoustic performance of a vehicle body in the low frequency range (i.e. [0-100] Hz). In this section the focus is to describe the application of those FE-based techniques and the numerical models.

A bead optimization application and validation case has been worked out for a vehicle-like model (denoted as the Concrete Car model in the remainder of this paper) [19], a simplified car cavity with the dimensions of a typical station wagon car cabin [8].

3.1 Vibro-Acoustic FE model

In order to test the proposed methodology, an FE vibro-acoustic model has been built up, in line with the main features of the Concrete Car, above presented.

The model consists of two coupled domains – the structural domain and the acoustic domain. The structural model has been made of steel with a shell thickness of 10mm, and it consists of a refined spare wheel panel (3.203 nodes, 3.166 quad elements) and the remainder of the concrete car (12.875 nodes, 12.787 quad elements). The spare wheel panel is a part of the vehicle floor panel, located at the rear of the Concrete Car model (see Figure 3 on the left). The vertical direction corresponds to the z-axis. The y-axis is in the longitudinal direction, and the x-axis is in the transversal direction of the vehicle.

The two structural components have been assembled with 72 rigid connections between coincident nodes; i.e. there are 432 (= 6 dofs/node x 72 nodes) junction DOFs. On the structural model, the locations of the 4 wheels have been defined; at the wheel center nodes, all DOFs are constrained except the rotation around the wheel axis (rx, i.e. the rotation around the global x-axis).

An eigenvalue analysis (Nastran SOL103) on the structural model has been performed yielding 43 natural modes in the frequency range of interest (i.e. up to 100 Hz). In order to take into account structural dissipative effects, a modal damping of 1% has been applied to all structural modes.

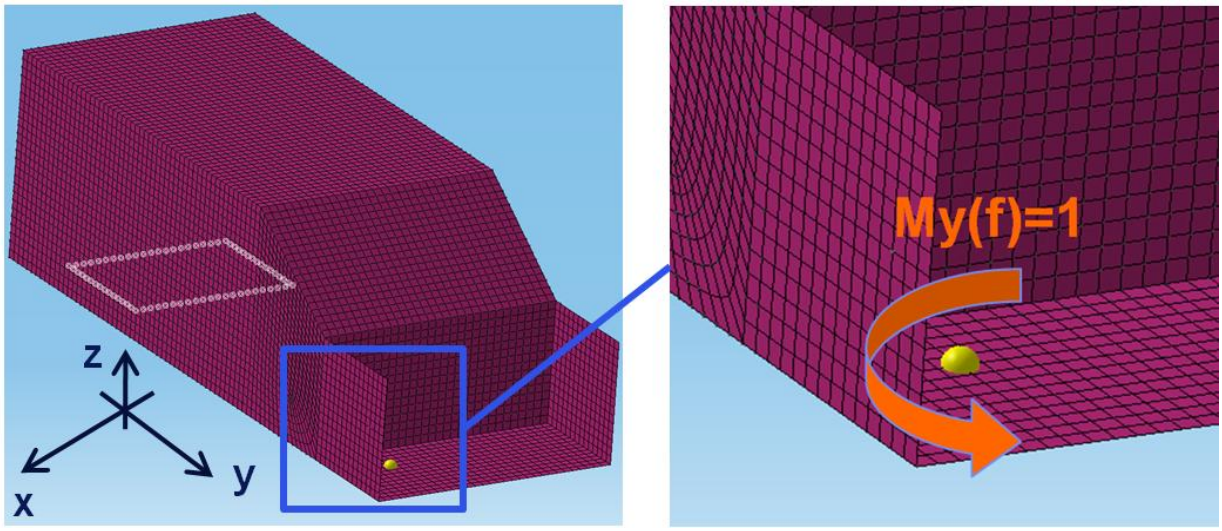

Figure 3. Structural model and load at the engine mount position

The vibro-acoustic cavity is filled with air, and modeled with 7.136 fluid elements (Nastran CHEXA elements) and 8.364 nodes. A virtual microphone is placed in the cavity near the virtual driver ear position. A modal analysis has been performed on the acoustic model yielding 3 modes in the frequency range of interest. The first acoustic natural mode is at 0 Hz, the second is at 52Hz and the third is at about 100Hz. In order to consider the dissipative effects due to the trim material, modal damping of 2% has been added.

A vibro-acoustic forced response case has been defined for the concrete car model. The Noise Transfer Function (NTF) of interest is the pressure over force resulting from a unit-magnitude moment input at DOF ry (i.e. the rotation around the global y-axis) at the concrete car engine mount, in the range [0, 100] Hz. A modal-based forced response strategy is used, consisting of calculating first the structural modes, followed by a forced response in the modal domain [20], and finally the propagation into the acoustics domain using the ATV approach.

3.2 Structural FE model – WBS-assembly level

The aim of the bead optimization is to reduce the acoustic radiation from the spare wheel panel, by applying a bead pattern. To speed up the iterations, a wave-based substructuring (WBS) approach is used to isolate the critical panel (which is kept in full FE representation) from the remainder of the vehicle (which is kept as a reduced modal model).

The idea behind Wave-Based Substructuring (WBS) is to achieve an efficient representation of the interface between the two coupled substructures, spare wheel panel and remainder. The wave calculation (see Section 2.1), involves a nominal FE model containing the spare wheel panel in its initial configuration. Aimed at reaching an assembly model for analyses up to 100Hz, the so-called wave-functions are calculated by using all the natural modes up to 150 Hz (i.e. 59 modes). The coupling between the two substructures is made by means of 59 wave participation factors, instead of 432 physical DOFs, as shown in Figure 4.

$$\left\{x_j^{(s)}\right\} = [W^{(s)}] \cdot \left\{p_1^{(s)}\right\} \tag{4}$$

The next step consists in the reduction of the remainder, for which the natural modes up 160 Hz are calculated. To improve the dynamic representation of the remainder, a set of residual attachment modes is added [14,15]. Usually one has to calculate the residual attachment modes for each of the physical junction DOFs, whereas in WBS they only need to be calculated for each of the wave DOFs, which drastically reduces the computational costs in the reduction procedure. The rigid connection between the

wave participation factors of both Substructures (A) and (B) in Figure 4 and Eq. (5), defines both the continuity and equilibrium conditions at the interface [12,13].

$$\left\{p_1^{(s)}\right\} = \left\{p_2^{(s)}\right\} \tag{5}$$

The dynamics of the achieved WBS-assembly model has been validated in terms of natural frequencies and MAC values aimed at comparing the mode shapes [7,8].

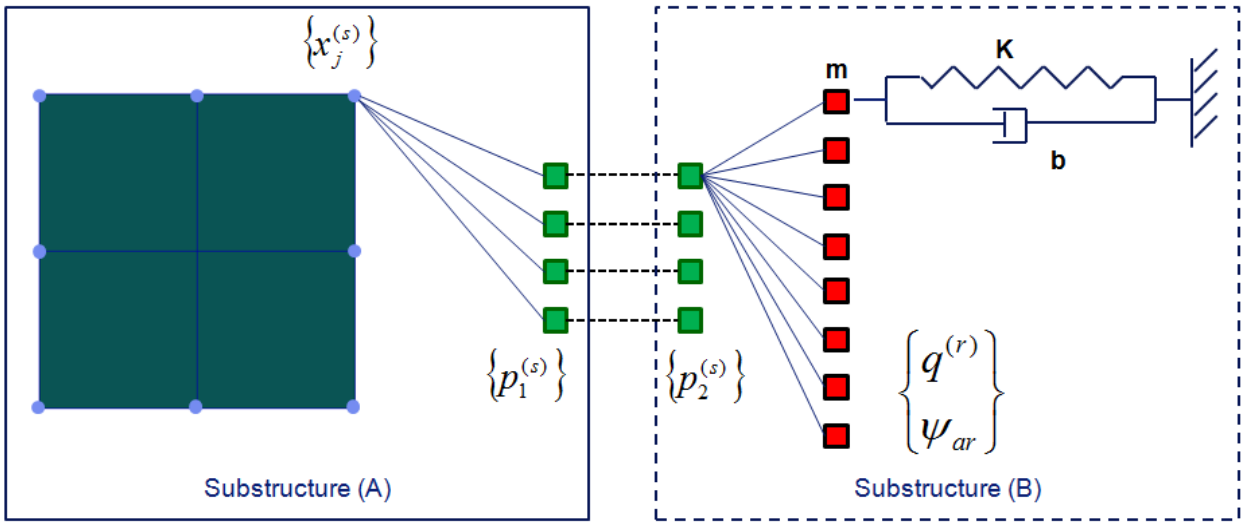

Figure 4: WBS-assembly model. Substructure A in FE representation on the left and Substructure B (reduced) on the right side. Connection between substructures using wave-DOFs.

An assembly-level FE model is now achieved, which consists in two substructures connected to each other by means of wave-DOFs. Furthermore, Wave-Based Substructuring allows re-writing the acoustic pressure at the virtual driver ear position in Eq. (2) as follows:

$$p(f) = \{MATV(f)\}_{REM}^{T} \cdot \{q(f)\}_{REM} + \{MATV(f)\}_{SWP}^{T} \cdot \{q(f)\}_{SWP} \tag{6}$$

where the total pressure is split into two contributions from the remainder and the spare wheel panel, respectively. The computationally most demanding step is the calculation of the Modal Acoustic Transfer Vectors for the remainder, which is calculated only once as it does not change w.r.t. modifications on the spare wheel panel. Calculation of the other 3 terms in eq. (6) is very fast.

4 Bead optimizations – Results

The optimizations presented in this section involve the critical sub-component (i.e. the spare wheel panel) located on the rear bottom area of the concrete car model, as shown in Figure 3. In the nominal model, the spare wheel panel is completely flat and its surface covers 3.5% of the total radiating surface. The vibro-acoustic contribution of the panel to the Noise Transfer Function (NTF) has been calculated up to 100Hz, according to Eq. (6).

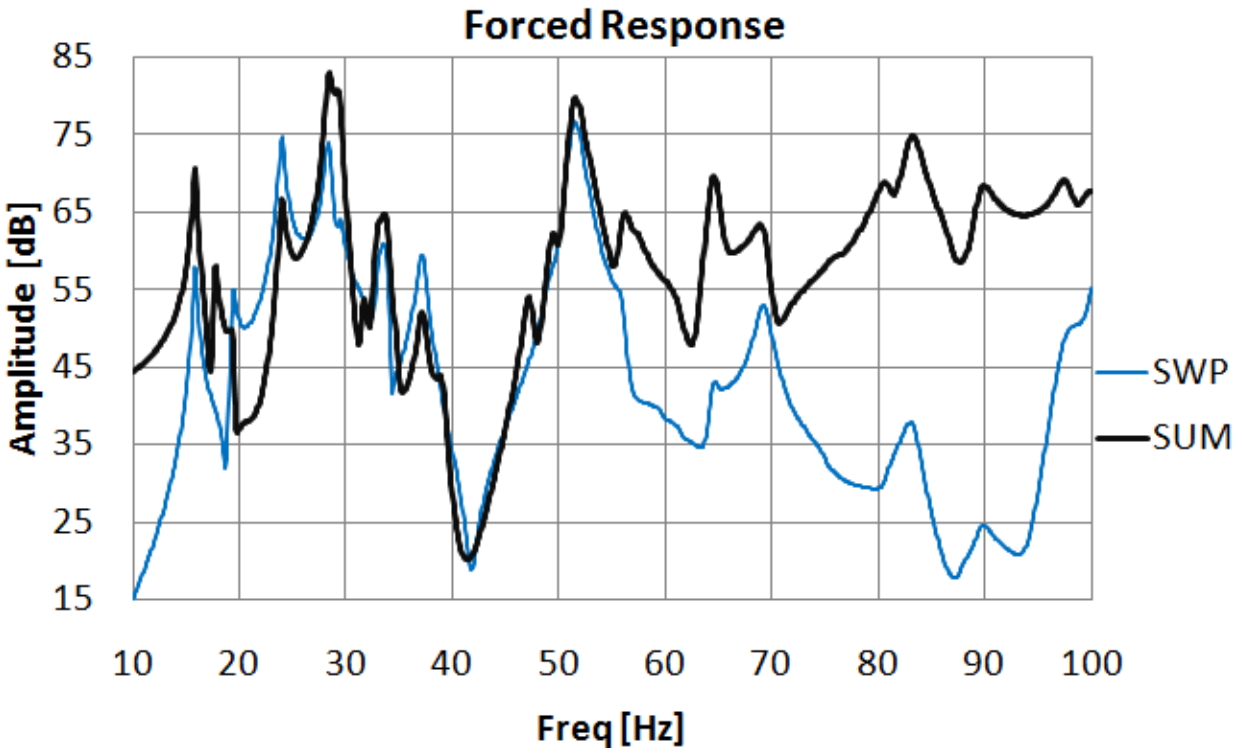

Figure 5: Noise Transfer Function for the nominal case. Total contribution (thick black line) and spare wheel panel contribution (thin blue line)

Figure 5 shows the Noise Transfer Function in dB ($p_{ref} = 2 \cdot 10^{-5}$ Pa) with a special focus on the spare wheel panel contribution (thin blue line). Despite its limited dimensions (as compared to the entire radiating surface), its contribution to the overall pressure is substantial in the lower frequency range up to 55 Hz. Figure 5 also shows that the radiated pressure by the panel may be higher than the sum (in terms of amplitude level), so that in the summation there is radiation from other panels with an opposite phase, thus reducing the total sum. In the higher frequency range (i.e. from 55 Hz up to 100 Hz) the panel contribution is less significant or even negligible.

The NVH behavior related to each modified version of the panel is compared by means of the Noise Transfer Function calculated up 100 Hz. The goal of the optimizations is to reduce the acoustic pressure in the virtual simulation environment, focusing on the main resonance peaks – in particular the peak at 51.5 Hz, which is predominantly due to both the high density of structural modes and the second acoustic mode. For this reason, the pressure decrease as compared to the nominal case has been used as objective for the first case. Furthermore, the frequency range of interest has been divided into 3 sub-ranges, in which the ratio between the widths of adjacent ranges has been kept constant in a logarithmic scale (i.e. $10^{1/3}$).

The time-harmonic acoustic pressure is given by

$$p(f,t) = \sqrt{2} \cdot p_{rms}(f) \cdot \cos[2\pi \cdot f \cdot t + \varphi(f)] \tag{7}$$

in which $\sqrt{2} \cdot p_{rms}(f)$ is the amplitude of the pressure at the frequency f.

In order to obtain a global parameter, the root mean square value in the frequency domain has been calculated according to

$$p_{RMS} = \sqrt{\int_{f_i}^{f_j} \left\| p_{rms}(f) \right\|^2 \cdot df} \tag{8}$$

Here, f_i and f_j are the boundaries of each considered frequency band.

Finally the Sound Pressure Level has been calculated in dB ($p_{ref} = 2 \cdot 10^{-5}$ Pa).

In Section 2, the concept of beading has been illustrated, focusing on the stiffening effect on the panel on which the bead modifications are applied. From a purely theoretical viewpoint, the best solution is reached when the sub-component is infinitely stiff. This condition is obtained when the height of the introduced bead patters tends to infinity.

All the performed optimizations have as design variable the nodal position of all the nodes that belong to the panel mesh. From this set, the boundary nodes must be excluded, since the mesh continuity between the remainder and the panel must be preserved. Aimed at avoiding geometrical issues during the calculation, an envelope surface has been introduced, which limits the bead patterns in practice to a certain maximal dimension. For this purpose, a special option in Tosca (called Penetration Check) in the optimization cycle has been enabled, to ensure that the beads never penetrate through the envelope mesh. This ensures that the bead patterns are of controlled finite dimension, so that a realistic bead pattern is obtained.

Figure 6 illustrates the envelop surfaces that have been used. This geometrical entity consist of two symmetric panels (the first located over the spare wheel panel and the second below) which allow a maximum bead height of 50mm. These surfaces have been used for all optimization analyses presented in this paper, so that the same kind of 'geometric reality check' is applied for each of the various bead pattern, generation algorithms and analysis runs.

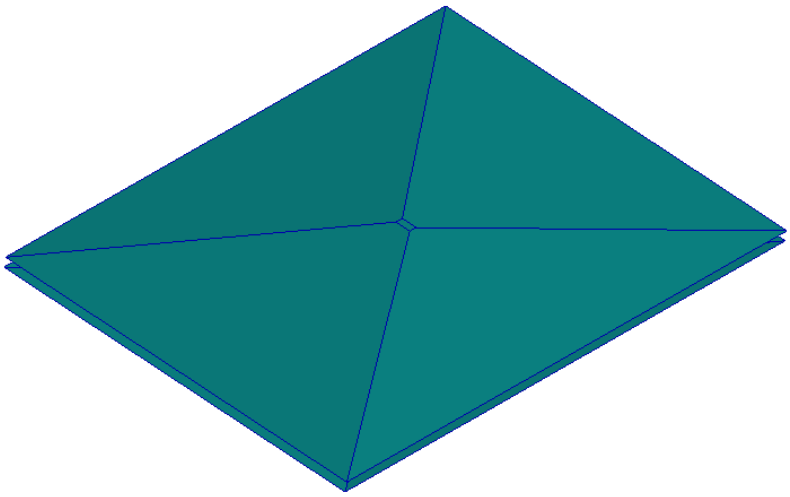

Figure 6: Envelop surface used to limit the height of the generated bead patterns.

4.1 Controller-based optimization in Modal Analyses

In this section, the Controller-based Algorithm [25] is used to re-shape the spare wheel panel. The controller-based algorithm can rely on a small set of design responses and analyses and it provides a strong control on the geometry of the generated patterns. The height of the beads can be specified as a design constraint by introducing the envelope surface, while the desired bead width has been varied from a minimum allowed value (i.e. 3 times the characteristic length of the shell elements) up to 0,32 m (i.e. 50% of the smallest dimension of the panel itself). A sensitivity analysis has been performed to evaluate the bead dimensions in the allowed design space, which has indicated that the best (vibro-acoustic) performance is obtained for small bead widths, even as low as below 0,1 m.

A suitable objective function for the controller-based optimization, is to maximize (or minimize) the natural frequencies of some selected modes. Assuming that the acoustic response can be considered as a weakly-coupled propagation of the structural response, the idea is to modify the structure in order to get benefits from the shifting of the natural modes.

For this purpose, the selection of a set of modes to be maximized is the crucial step. The selection has been made by using three different methods, below reported:

a) Modes with high displacement in correspondence of the spare wheel panel, as proposed by Donders et al. [8]: This condition is often reached by selecting low-frequency modes, which have a considerable impact on the panel structural dynamics, also shown by Blanchet et al. [27].

b) Frequency approach: Given a frequency range in which the acoustic pressure is to be reduced, one can shift the natural frequencies related to the modes that give the most significant contribution (in terms of acoustic pressure). The rationale is that by shifting (towards either higher or lower frequencies) the peaks of the closest modes to frequency of interest, one obtains a local modification of the noise transfer function.

c) MAC (Modal Assurance Criterion) autocorrelation: As previously mentioned, the controller algorithm creates beads aimed at stiffening the structure for the selected (modal) shapes. If modes are selected that are weakly correlated (in terms of modal shapes), the applied structural modification results in a stiffening effect for different modal shapes, thus having an impact on a wider frequency range.

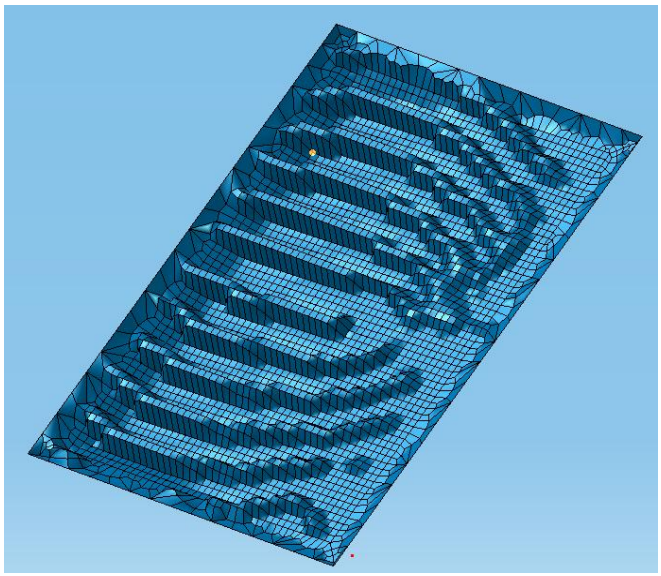

Figure 7: Best case obtained with bead controller algorithm based on eigenanalyses

Figure 7 shows the best bead pattern obtained by using the controller algorithm, in terms of NVH performance. It can be seen that well defined bead patterns have been created. The objective has been defined by selecting the structural modes #4, #13, #19 as target, for which the eigenfrequency had to be maximized. The best results have been obtained by using a bead width of 50mm, which is the minimum allowed when considering the average length of the finite elements that have been used. Here it is noted that from a practical engineering viewpoint, a smaller bead width is not desirable, since very small beads are more challenging to manufacture and to use in the eventual product (e.g. sharp edges are not desirable, narrow beads are not desirable since dust & dirt will stick in between, …)

4.2 Sensitivity-based optimization in Forced Responses

The structural optimization based on modal-based forced responses allows optimizing the spare wheel panel in the same condition as in the nominal case (load, constraints, damping, etc.). For this purpose, a forced analysis has been defined in order to perform the noise transfer function up to 100 Hz. Two different damping models have been evaluated, namely structural (material) damping and modal damping. Both yield very similar results in terms of final NVH behavior. The vibro-acoustic response has been obtained by means of modal superposition, supported by the calculation of the modal participation factors for the WBS-assembly FE model.

Eq. (9) shows the modal participation factors, where $\{\Phi_j\}$ is the *j*th normal mode calculated on the WBS-assembly model, $\{F\}$ is the load vector and β represents the damping effect ($\beta = 2 \cdot \xi$ for structural damping and $\beta = 2 \cdot \xi \cdot \frac{\omega}{\omega_{nj}}$ for modal damping, where ξ is the critical damping ratio).

$$q_j(\omega) = \frac{\{\Phi_j\}^T \cdot \{F\}}{\omega_{nj}^2 \cdot (1 - \left(\frac{\omega}{\omega_{nj}}\right)^2 + i \cdot \beta)} \tag{9}$$

The innovation presented in this paper is the vibro-acoustic optimization by combining a structural bead optimization methodology and a structural FE model with an acoustic target function. The acoustic pressure at the virtual driver ear position is given by Eq. (2), written as the product between the modal acoustic transfer vectors and the modal participation factors. Thus, the acoustic pressure is directly controllable by acting on the participation factors related to normal modes and residual attachment vectors.

The best NVH performance corresponds to minimizing the pressure response, see Eq. (10). By considering only a subset of modes (i.e. $j \in J$), the objective function $p(f)$ results in an estimation of the acoustic pressure

$$\min\{p(f)\} = \sum_j MATV_j(f) \cdot q_j(f) \tag{10}$$

In this paper the objective function has been minimized in correspondence of the second acoustic resonance, where a peak is shown in the NTF. Moreover the objective function is built up by using the MATV calculated upon the normal modes performed in the reduction step. In order to provide a better estimation of the panel radiation, the objective function in Eq. (11) has been enriched by adding a contribution based upon the structural response of the panel

$$\min\{p(f)\} = \sum_j MATV_j(f) \cdot q_j(f) + K \cdot 2\pi \cdot f \cdot x(f) \tag{11}.$$

Eq. (11) represents a more complete estimation, since the radiated noise from both panel and remainder are directly taken into account. Here, $2\pi \cdot f \cdot x(f)$ represents the velocity of a node that belongs to the panel mesh and *K* represents a scale factor which weights the two contributions to the total pressure, and depends upon both frequency range and the selected node.

Figure 8 shows the mesh configuration that leads to the best NVH performance in terms of both local pressure reduction and SPL calculated for the previously defined frequency sub-ranges. The objective function described in Eq. (11) leads to a better performance in terms of pressure reduction in correspondence of the peak at 51.5 Hz, but yields a lower performance for the other (global) parameters.

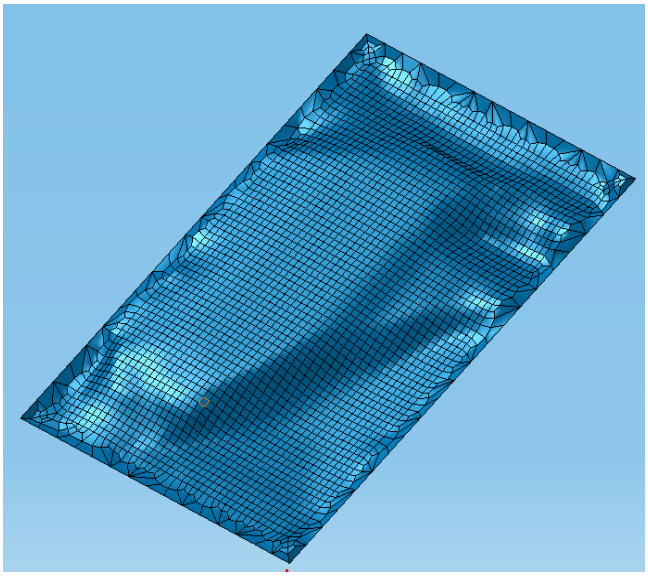

Figure 8: Best case obtained with bead sensitivity algorithm based on modal based forced response analyses

4.3 Comparison

The results obtained with both methods are compared and evaluated in this section. In view of deriving guidelines, the calculation time has been reported and the mass of the optimized panel has been observed. Since the FE model is modeled with shell elements, the estimation of the mass from a virtual model gives an indication regarding the quality of panel surface, and therefore gives a first view on its manufacturability.

All calculations have been performed on a CPU Intel Xeon 5150 computer system (Dual Core 2.66 GHz, RAM 8.0 GB RAM, 750 GB scratch space) running a Windows Server Standard SP2 x64 operating system, with MSC Nastran version 2005.5.2 [23] as FE solver, using LMS Virtual.Lab [24] for vibro-acoustic ATV calculations and file pre- and post processing and using Tosca [25] to run structural optimization analyses.

Figure 9 shows the noise transfer function for the spare wheel panel in its original configuration and the vibro-acoustic response that is obtained for each of the two optimized bead shapes in Figure 7 (Controller-based) and Figure 8 (Sensitivity-based). Note that the NTFs related to the optimized shapes are very similar, especially in correspondence of the main resonance peaks. The application of bead patterns on the panel results in a stiffening effect, which leads to an upward shifting of the natural frequencies and consequently of the resonance peaks. The most significant reduction in terms of acoustic pressure is obtained at the main resonance peak (second acoustic mode). This peak has been lowered for both the bead patterns. Table 1 provides a numerical comparison between the NTF for the two optimized panels. Here, local reductions in pressure are reported as well as the global parameters (i.e. SPL).

In addition, also a non-NVH parameter has been used as a criterion to evaluate the performance of the two bead patterns, namely the mass of the panel, which can be calculated directly from the shell properties. The nominal spare wheel panel is flat, so that in the FE model the creation of the bead pattern leads to the increase of the shell surface and hence an increase in mass, which is +2.85% for the sensitivity algorithm and +37.88% for the application of the bead controller algorithm. Further research will investigate if a reduction of the panel thickness, to compensate the increased area, will influence the increased NVH performance. As such, although at this point both optimization approaches yield very similar results, compensating for the strong mass increase of the bead-controller approach with reducing the thickness might degrade the NVH performance again.

Finally it is noted that the shape obtained with the Sensitivity-based Algorithm is smoother and hence is easier to manufacture.

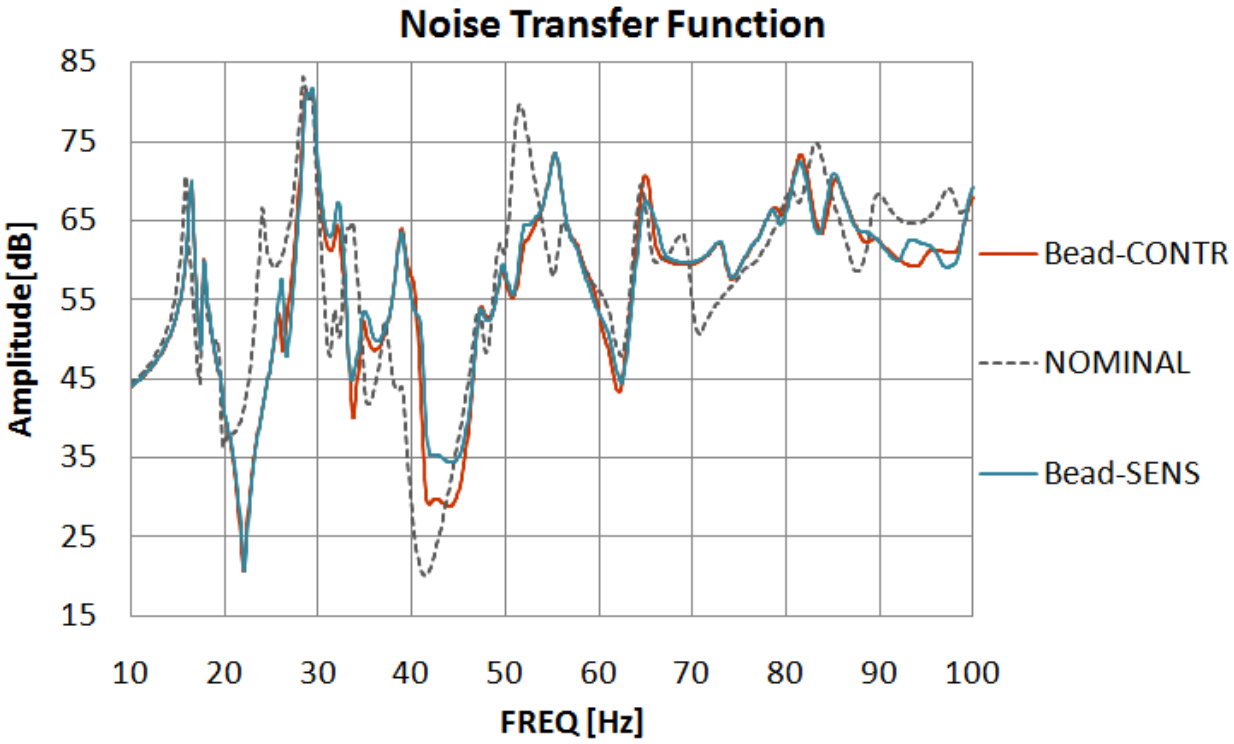

Figure 9: Noise Transfer Functions. Nominal Spare Wheel Panel (dashed grey), Optimized panel with Bead Controller (red line) and Optimized panel with Bead Sensitivity (blue line).

	Optimized panel (Controller and SOL103)	**Optimized panel (Sensitivity and SOL111)**	**Flat panel**
Iterations [#]	3	10	-
Calculation time	~ 100 sec.	~ 95 min.	-
SPL (Band 1) [dB]	64,41	64,55	**65,01**
SPL (Band 2) [dB]	79,66	79,53	**80,59**
SPL (Band 3) [dB]	78,99	78,83	**81,57**
SPL (all bands) [dB]	82,42	82,28	**84,17**
Δp at 51,5 Hz [dB]	-21,7	-18,82	-
Δp at new peak (~55Hz) [dB]	-6,14	-6,23	-
Panel's Mass [kg]	84,495	63,032	**61,282**

Table 1: Solution parameters and obtained NVH performances

5 Conclusion

A methodology for NVH optimizations of vehicles in the low and medium frequency range has been presented. The focus of the presented work has been on the coupling between vibro-acoustic FE models and an optimization program that provides purely structural design response calculations and structural bead patterns. For a vehicle-like case, the interior acoustics comfort has been improved by means of structural bead modifications applied on a critical component (i.e. the spare wheel panel).

A so-called Wave-Based Substructuring (WBS) approach has been used to achieve an efficient FE model, to reduce the burden in the reduction step and to facilitate the coupling between substructures at an assembly level. By means of a (Modal) Acoustic Transfer Vector approach, efficient acoustic pressure response predictions as a result of structural modifications can then be obtained.

The main challenge has been the optimization of the interior vibro-acoustic response by relying on an optimization approach which considers only structural response objectives (i.e. taken from modal analyses and forced response analyses) as a basis for bead pattern creation.

The main innovation of the presented work consists in a technique which is based on (structural) forced response analyses. An estimation of the acoustic pressure, at the virtual driver ear position, has been set as objective function. This objective has been written as function of the modal participation factors and the velocities at strategic points of the panel.

Future research will focus on investigations to keep the bead panel mass constant and on the application of the presented methodology on industrial cases.

Acknowledgements

The authors kindly acknowledge the European Commission for supporting the EC Marie Curie RTN “Smart Structures”, from which the first author holds an ESR training grant, and for supporting the collaborative project “MID-MOD - Mid-frequency vibro-acoustic modelling tools”. Furthermore, we gratefully acknowledge IWT Vlaanderen for supporting the IWT O&O project “MIDAS - next generation numerical tools for mid-frequency acoustics”. Finally, we would like to thank FE Design GmbH for their contribution to this research activity.

References

[1] H. Van der Auweraer, J. Leuridan, *The New Paradigm of Testing in Today’s Product Development Process*, Proc. ISMA2004, Leuven, Belgium, Sept. 20-22, 2004, pp. 1151–1170.

[2] D. Roesems, *A new methodology to support an optimized NVH engineering process*, Sound and Vibration, 31(5):36–45, 1997.

[3] G. Wöhlke, E. Schiller, *Digital Planning Validation in automotive industry*, Computers in Industry, 56(4):393–405, 2005.

[4] M. Shephard, M. Beall, R. O’Bara, B. Webster, *Toward simulation-based design*, Finite Elements in Analysis and Design, 40(12):1575–1598, 2004.

[5] H. Shiozaki, Y. Kamada, S. Kurita, S. Goossens, J. Van Herbruggen, V. Cibrario, and L. Poppelaars, *CAE based vehicle development to reduce development time*, Proc. JSAE, Yokohama, Japan, 2005.

[6] R. Hadjit, M. Brughmans, H. Shiozaki, *Application of Fast Body Optimization Procedures to Shorten Car Development Cycles*, Proc. JSAE, Yokohama, Japan, 2005.

[7] S. Donders, *Computer-aided engineering methodologies for robust automotive NVH design*, PhD thesis, K.U.Leuven, Department of Mechanical Engineering, Division PMA, Leuven, Belgium, February 2008. Available online: http://hdl.handle.net/1979/1698.

[8] S. Donders, L. Hermans, E. Nauwelaerts, S. Chojin, B. Pluymers, W. Desmet. *CAE Technologies for efficient Vibro-Acoustic Vehicle Design and Optimization*. Proceedings ISMA 2008.

[9] H. Van der Auweraer, S. Donders, R. Hadjit, M. Brughmans, P. Mas, J. Jans, *New approaches enabling NVH analysis to lead design in body development*, Proc. EIS NVH Symposium "New Technologies and Approaches in NVH", Coventry, UK, November 3, 2005.

[10] D. Mundo, A. Maressa, N. Rizzo, S. Donders, W. Desmet. *A database frame work for industrial vehicle body concept modeling*. WSEAS 2010.

[11] R. Guyan, Reduction of stiffness and mass matrices, *AIAA Journal* 3 (2) (1965), pp. 380–387

[12] R.R. Craig Jr., *Structural dynamics – an introduction to computer methods*, Wiley, NY, (1981).

[13] R.R. Craig, Jr. and M.C.C. Bampton. *Coupling of substructures for dynamic analyses*. AIAA Journal, 6(7):1313–1319, 1968.

[14] R.H. MacNeal, *A hybrid method of component mode synthesis*, Comput Struct 1 (1971), pp. 581-601.

[15] S. Rubin. *Improved Component-Mode Representation for Structural Dynamic Analysis.* AIAA Journal, 13(8):995–1006, 1975.

[16] S. Donders, R. Hadjit, M. Brughmans, L. Hermans, and W. Desmet. *A Wave-Based Substructuring Approach for Fast Modification Predictions and Industrial Vehicle Optimization.* In Proceedings of ISMA 2006, pages 1901–1912, Leuven, Belgium, 2006. Sept. 18-20.

[17] S. Donders, B. Pluymers, P. Ragnarsson, R. Hadjit and W. Desmet, *The Wave-Based Substructuring approach for the efficient description of interface dynamics in substructuring*, Journal of Sound and Vibration, Vol. 329, Issue 8, pp. 1062-1080, 2010.

[18] F. Gérard, M. Tournour, N. El Masri, L. Cremers, M. Felice, A. Selmane, *Numerical Modeling of Engine Noise Radiation through the use of Acoustic Transfer Vectors - A Case Study*, Proc. SAE 2001-01-1514, Traverse City, MI, USA, (2001).

[19] B. Pluymers, *Wave Based Modelling Methods for Steady-State Vibro-Acoustics*, PhD thesis, K.U.Leuven, Department of Mechanical Engineering, Division PMA, Leuven, Belgium, June 2006. Available online: **http://hdl.handle.net/1979/320**.

[20] W. Heylen, S. Lammens, P. Sas, *Modal Analysis Theory and Testing*, Katholieke Universiteit Leuven, Departement Werktuigkunde, Leuven (1997).

[21] L. Hermans, M. Brughmans, *Enabling vibro-acoustic optimization in a superelement environment: a case study*, Proc. IMAC XVIII, San Antonio, TX, USA, (2000), pp. 1146-1152.

[22] P. Clausen, C. Pedersen, *Non-parametric Large Scale Structural Optimization for Industrial Applications*, Proc. ECCM-2006, Lisbon, Portugal, June 5-8, 2006.

[23] MSC, *MSC.Nastran 2005.5.2*, (2005).

[24] LMS International, *LMS Virtual.Lab Rev. 8B-SL1*, April 2009.

[25] FE Design, *TOSCA Structure 7.0.1*. May 2009

[26] FE Design, Tosca Structure 7.0.1. User Manual. May 2009

[27] H. Van der Auweraer, T. Van Langenhove, M. Brughmans, I. Bosmans, N. El Masri, S. Donders, *Application of Mesh Morphing Technology in the Concept Phase of Vehicle Development*, Int. J. Vehicle Design, Vol. 43, Nos. 1-4, pp. 281-305, 2007.

[28] D. Blanchet, W. Van Hal, A. Cailled. *Effects of beading on Radiated Noise*. SAE International, 2010-01-1407.

[29] Pluymers, B., Van Hal, B., Vandepitte, D., Desmet, W. (2007). Trefftz-based methods for time-harmonic acoustics. *Archives of Computational Methods in Engineering, 14* (4), 343-381.

[30] P. Clausen, C. Pedersen, *Non-parametric NVH Optimization of Industrial Designs*, Proc. WCSMO-2009, Lisbon, Portugal, June 1-5, 2009.

[31] K.-U. Bletzinger, M. Firl, F. Daoud, *Approximation of Derivatives in Semi-analytical Structural Optimization*, III ECCM Lisbon, Portugal, 5-8 June, 2006

[32] K.-U. Bletzinger, F. Daoud, M. Firl, *Filter techniques in shape optimization with cad-free parametrization*, III ECCM Lisbon, Portugal, 5-8 June, 2006